Two-Channel Thermal Unimolecular Decomposition of Alkyl Iodides

Akira Miyoshi,* Noboru Yamauchi, Keishi Kosaka, Mitsuo Koshi, and Hiroyuki Matsui

Department of Chemical System Engineering, The University of Tokyo, 7-3-1 Hongo, Bunkyo-ku, Tokyo, 113-8656, Japan

Received: July 8, 1998; In Final Form: September 23, 1998

The competition between the C−I bond fission and the four-center HI elimination in the thermal unimolecular decomposition of C_3−C_4 alkyl iodides has been investigated at temperatures of 950−1400 K and pressures around 1 atm by a shock tube technique. The concentration of iodine atoms was followed by atomic resonance absorption spectrometry. For primary iodides, the absolute rate constants were measured at temperatures of 950−1100 K. The branching fractions for C−I bond fission channels were determined for all isomers of C_3 and C_4 alkyl iodides at temperatures of 950−1400 K. A drastic change in the branching fraction for the C−I bond fission channel was observed from primary iodides (0.6−0.9) to secondary iodides (0.2−0.4), and further to tertiary iodide (<0.05), which was mainly ascribed to the lowering of the threshold energy for the HI elimination channel from primary to secondary (by ∼14 kJ mol^{-1}) and from secondary to tertiary (by ∼20 kJ mol^{-1}) iodides. The α-CH_3 substituent effect to the activation energy was in good accordance with previous investigations. The observed temperature dependence of the branching fraction could not be explained by the simple high-pressure limit treatment, and an RRKM analysis showed that the proper treatment of the mutual effect of two dissociation channels is essentially important to reproduce the observed branching fractions and their temperature dependence. A simple interpretation for the α-CH_3 substituent effect is presented in terms of the avoided intersection between ionic dissociation (RI → $R^+ + I^-$) surface and the repulsive surface of HI approach to the double bond.

Introduction

The four-center molecular elimination is a frequently observed phenomenon in the unimolecular dissociation of hydrocarbons. Especially, the molecular elimination from halocarbons has been widely studied in various points of view. Because the molecular elimination process involves a high barrier other than the enthalpy change of the reaction, the internal or translational excitation of the products is expected and nonstatistical energy distribution may be also expected. Spontaneous[1] or laser[2] emission from the vibrationally excited products (for example, HF up to $v = 4$) has been observed in chemical activation or infrared mutiphoton activation. Internal[1,2] and translational[3] energy partitioning has been the subject of many studies and the main interest has been focused on the dynamics of the exit channel and the comparison with the statistical theory.

The nature of the transition state for the four-center molecular HX (hydrogen halide) elimination reaction from haloalkanes has been extensively discussed.[4] The activation energy has been shown[5] to decrease by about 29 kJ mol^{-1} for each α-CH_3 substitution, which is in good accordance with the classical Markovnikov selection rule for the reverse HX addition reaction to alkenes. Since such a large effect to the activation energy could not be expected from the energetics of neutral reactants and products, Maccoll and Thomas[6] first suggested a relation with the heterolytic dissociation (RX → $R^+ + X^-$) energy, which decreases by about 0.9 eV (∼ 87 kJ mol^{-1}) for each α-CH_3 substitution. This model was subsequently refined by Benson, Bose, and Haugen[5,7] as the semi-ion-pair model, which assumes a more realistic, less polarized semi-ion-pair transition state. Later, many experimental investigations were reported in relation to this subject. Since the heterogeneous effect had been thought to be the source of the large scatter in earlier experimental data, Tsang[8] reported reliable Arrhenius parameters from single-pulse shock tube experiments, which were free from the heterogeneous effect. He also showed the correlation between the activation energy and the heterolytic dissociation energy. Tschuikow-Roux and co-workers[9] reported shock tube studies for fluoroethanes and developed a modified semi-ion-pair model[10] for various substituted haloalkanes. Setser and co-workers[11] reported extensive investigations by the chemical activation method. In combination with the detailed RRKM model, they derived the threshold energies for the four-center HX elimination reactions and the averaged energy removed per collision. Some modifications to the semi-ion-pair model were reported to be necessary for the interpretation of the experimental results. More recently, Holmes and co-workers[12] reported chemical activation investigation and explained the substituent effect in terms of the charge separation in the transition states. Although some modifications have been made, the "semi-ion-pair" treatment of the transition state has been successful for various substituted haloalkanes.

Several ab initio calculations have been also reported for the four-center HX elimination processes. Kato and Morokuma[13] reported a detailed theoretical investigation on the intrinsic reaction coordinate (IRC) of HF elimination from fluoroethane. Their investigation was focused on the structure of the transition state and exit channel IRC in relation to the experimentally observed vibrational excitation of HF. Although a comparison of the transition-state geometry with the previous models was made, no analysis on the polarization of the transition state was reported. Recently, Toto et al.[14] reported a detailed analysis of the charge distribution of the transition states and the F− or Cl− substituent effect for HF and HCl elimination processes. Although some polarization exists in the transition states, no

10.1021/jp982915u CCC: $18.00
Published on Web 12/17/1998

systematic correlation was found between the polarization and the stabilization energy of the transition states, and they concluded that a simple model for the substituent effect remains to be developed.

For alkyl iodides, since the C−I bond is weak, the simple C−I bond fission reactions are known to compete with the molecular elimination processes and were speculated to be the source of the complexity in earlier measurements.[5] However, the experimental investigation on the simple bond fission channel is limited, mainly because of the experimental difficulty induced by the complex radical chain reactions. From the theoretical point of view, the experimental investigation on the competition between two dissociation channels is interesting since the branching fraction is expected to be very sensitive to the energy-transfer phenomenon at the high-energy regime around the dissociation thresholds.[15] The alkyl iodide is one of the suitable candidates for the investigation of the two-channel effect in the thermal unimolecular reactions since the threshold energies for competing HI elimination and C−I fission processes are close to each other. King et al.[16] reported a very low pressure pyrolysis study on the *n*- and *i*-propyl iodides. For *n*-propyl iodide, the competition of the C−I bond fission channel was observed and a two-channel RRK calculation was performed to analyze the experimental results. Hippler et al.[17] studied the thermal decomposition rate constants for *tert*-butyl iodide and *tert*-butyl bromide in order to investigate the possible contribution of the second dissociation channel, although no such effect could be found in the experimental results. More recently, Kumaran et al.[18] reported a study on the thermal decomposition of ethyl iodide. The overall rate constant and the branching fraction for C−I fission channel were determined by a shock tube with ARAS (atomic resonance absorption spectrometry). The experimental results were analyzed by RRKM calculations with a steady-state solution of the master equation for the two-channel problem. However, the experimental investigation has been limited to primary iodides only.

In the present study, the thermal decomposition of a series of alkyl iodides including primary, secondary, and tertiary iodides (*n*-C_3H_7I, *i*-C_3H_7I, *n*-C_4H_9I, *s*-C_4H_9I, *i*-C_4H_9I, *t*-C_4H_9I) has been studied by a shock tube technique. Competition between the C−I bond fission and HI elimination reactions was monitored by observing the iodine atom concentrations by ARAS at temperatures of 950−1400 K. Experimental results were analyzed with an RRKM calculation with proper treatment of the mutual effect of two dissociation channels. A simple interpretation is presented for the α-CH_3 substituent effect to the threshold energy for the HI elimination processes.

Experimental Section

All experiments were performed with a diaphragmless stainless steel shock tube equipped with an ARAS detection system. The detail of the apparatus has been described elsewhere.[19] Sample gas mixtures of alkyl iodide largely diluted in Ar (1−10 ppm) were heated behind the reflected shock waves and the concentration−time profiles of product iodine atoms were measured by ARAS. Resonant radiation of iodine atom at 183.0 nm [$^4P_{5/2}-^2P_{3/2}$ (6s−5p)] emitted from a microwave discharge of a flowing I_2/He (0.1%) mixture was used as the light source for ARAS.

The branching fraction for the C−I bond fission channel was determined by the quantitative concentration measurement of I atoms. The concentration versus absorbance calibration curve was constructed by using the thermal decomposition of methyl iodide,

$$CH_3I + M \rightarrow CH_3 + I + M \quad (1)$$

The constructed calibration curves are shown in Figure 1. Slight density dependence was observed, probably due to the pressure broadening of the line shape of the absorber atom in the shock tube. No evident temperature dependence was observed, probably because the pressure broadening dominates over the Doppler broadening for such a heavy atom.

Preliminary experimental investigations were performed for the thermal decomposition of the ethyl iodide,

$$C_2H_5I + M \rightarrow C_2H_5 + I + M \quad (2a)$$

$$\rightarrow C_2H_4 + HI + M \quad (2b)$$

which has been extensively investigated by Kumaran et al.[18] The derived branching fraction for C−I fission pathway (2a) was temperature independent and was 0.92 ± 0.06. The present result is in good agreement with the results obtained by Kumaran et al.,[18] 0.89 ± 0.07, obtained from the I atom measurements.

The overall rate constants were measured for primary iodides in the temperature range 950−1100 K. The branching fractions were measured in the temperature range 950−1400 K. Experimental results were obtained mostly around the total pressure of 1.0 atm (buffer gas is Ar). For some experiments, it was varied from 0.6 to 1.9 atm in order to investigate the pressure effect.

Gases used were obtained from Nihon Sanso (He, >99.9999%; Ar, >99.9999%), Wako (I_2, 99.9%; CH_3I, >99%; *n*-C_3H_7I, >97%; *i*-C_3H_7I, >99%), and Tokyo Kasei (C_2H_5I, >99%; *n*-C_4H_9I, >98%; *s*-C_4H_9I, >97%; *i*-C_4H_9I, >97%; *t*-C_4H_9I, >95%). All reagents were purified by trap-to-trap distillation. Ar was purified by passing through a cold trap (−140 °C). Indicated error limits for the experimental results are at the two standard deviations level.

Results

In the present study, the thermal decomposition of two isomers of propyl iodides and four isomers of butyl iodides has been investigated.

$$n\text{-}C_3H_7I + M \rightarrow n\text{-}C_3H_7 + I + M \quad (3a)$$

$$\rightarrow C_3H_6 + HI + M \quad (3b)$$

$$i\text{-}C_3H_7I + M \rightarrow i\text{-}C_3H_7 + I + M \quad (4a)$$

$$\rightarrow C_3H_6 + HI + M \quad (4b)$$

$$n\text{-}C_4H_9I + M \rightarrow n\text{-}C_4H_9 + I + M \quad (5a)$$

$$\rightarrow 1\text{-}C_4H_8 + HI + M \quad (5b)$$

$$s\text{-}C_4H_9I + M \rightarrow s\text{-}C_4H_9 + I + M \quad (6a)$$

$$\rightarrow 2\text{-}C_4H_8 \text{ (or } 1\text{-}C_4H_8) + HI + M \quad (6b)$$

$$i\text{-}C_4H_9I + M \rightarrow i\text{-}C_4H_9 + I + M \quad (7a)$$

$$\rightarrow i\text{-}C_4H_8 + HI + M \quad (7b)$$

$$t\text{-}C_4H_9I + M \rightarrow t\text{-}C_4H_9 + I + M \quad (8a)$$

$$\rightarrow i\text{-}C_4H_8 + HI + M \quad (8b)$$

A typical time profile of the I atom concentration is shown in Figure 2. For primary alkyl iodides, the overall rate constants were determined from the growth of the iodine atom concentra-

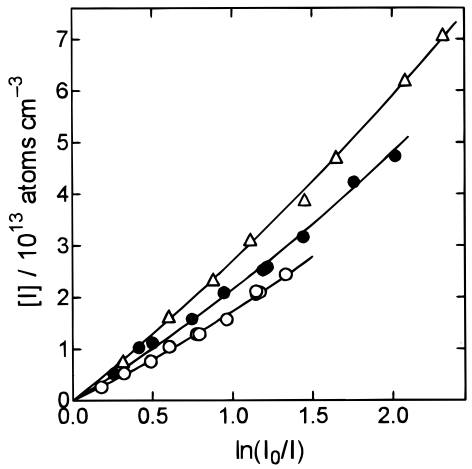

Figure 1. Absorbance [ln(I_0/I)] versus concentration calibration curves for I atom ARAS. Open triangles (△), closed circles (●), and open circles (○) denote the experimental data obtained at total densities of 15.6×10^{18}, 10.4×10^{18}, and 5.2×10^{18} molecules cm^{-3} (Ar), respectively. Solid lines denote the results of least-squares fitting to second-order polynomial.

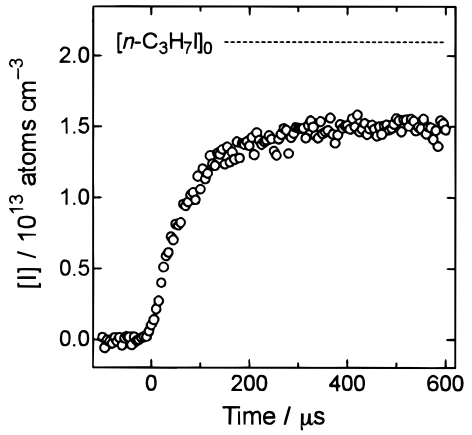

Figure 2. An example of the I atom concentration−time profile observed in the thermal decomposition of *n*-C_3H_7I. Experimental conditions are as follows: $T = 1039$ K, total density $= 7.03 \times 10^{18}$ molecules cm^{-3}, and sample gas composition = *n*-C_3H_7I (2.98 ppm)/Ar. Dotted line is drawn to indicate the initial concentration of *n*-C_3H_7I.

tion by fitting to the function

$$[\mathrm{I}] = A[1 - \exp(-k_\mathrm{I}\, t)] \tag{9}$$

where k_I is the first-order overall rate constant. For secondary and tertiary iodides, the rate constants could not be measured because the rate constants were too large and the branching fractions for I atom formation were small as will be described below. The branching fraction for the C−I bond fission channel was determined from the plateau of the iodine atom concentration as is observed in Figure 2. In the experiments for *i*-C_3H_7I, a gradual rise of the I-atom concentration was observed due to the reaction

$$\mathrm{H} + \mathrm{HI} \rightarrow \mathrm{H_2} + \mathrm{I} \tag{10}$$

since a significant amount of HI is formed by reaction 4b and hydrogen atoms are formed by the thermal decomposition of the *i*-C_3H_7 radical,

$$i\text{-}\mathrm{C_3H_7} + \mathrm{M} \rightarrow \mathrm{C_3H_6} + \mathrm{H} + \mathrm{M} \tag{11}$$

following reaction 4a. To minimize this effect, low concentration (1−2 ppm) sample gas was used especially for *i*-C_3H_7I. For other alkyl iodides, the effect of reaction 10 was smaller because of the lower HI yield and/or the lower yield of H atom from the subsequent thermal decomposition of alkyl radicals.

Measured first-order rate constants for primary alkyl iodides (*n*-C_3H_7I, *n*-C_4H_9I, and *i*-C_4H_9I) were summarized in Figure 3. For *n*-C_3H_7I, the pressure dependence of the rate constant was investigated under total pressures from 0.64 to 1.91 atm. No significant pressure effect was observed. The rate constants are supposed to be in, or close to, the high-pressure limit. For primary iodides, since the higher C−I fission channel is already dominant as shown below, the pressure effect to the overall rate constant is expected to be smaller for larger molecules. (This was also verified by the RRKM calculation described below.) Thus, for larger alkyl iodides, the rate constant measurements were done at pressure around 1.0 atm only.

Measured branching fractions for C−I bond fission channels ($f_{\mathrm{C-I}}$) are summarized in Figure 4. A clear difference was found among primary (*n*-C_3H_7I, *n*-C_4H_9I, and *i*-C_4H_9I; $f_{\mathrm{C-I}} = 0.6-0.9$), secondary (*i*-$C_3H_7I$ and *s*-C_4H_9I; $f_{\mathrm{C-I}} = 0.2-0.4$), and tertiary (*t*-$C_4H_9I$; $f_{\mathrm{C-I}} < 0.05$) iodides. Almost no temperature dependence was found for primary iodides, but slight temperature dependence was found for secondary and tertiary iodides. The extremely small branching fraction for *t*-C_4H_9I should be discussed carefully since the observed iodine atoms (∼3%) may be ascribed to the impurity (probably the other isomers of alkyl iodides) considering the specified purity (>95%) of the reagent used. No apparent pressure effect to the branching fractions was found for *n*-C_3H_7I. For other iodides, the experiments were done at a pressure around 1.0 atm only, since the RRKM calculation (described below) predicts the very small pressure effect to the branching fractions.

Discussion

The overall rate constants for primary iodides were found to be close to each other in the temperature range studied, 950−1100 K, as shown in Figure 3. This implies the similarity of the Arrhenius parameters for C−I bond fission channels. Since, as shown in Table 1,[20−23] no systematic change in the C−I bond dissociation energy was found from primary to tertiary iodides, the activation energy for C−I bond dissociation channels can be estimated to be nearly constant for all alkyl iodides. Thus, the drastic change in the branching fractions from primary to tertiary iodides must be ascribed to the significant change in the activation energy and/or activation entropy (including the reaction path degeneracy) for the four-center HI elimination channels.

A. High-Pressure Limit Analysis. A simple high-pressure limit analysis was made as a first step, to derive the activation energy by using the calculated preexponential factor. Transition state theory (TST) calculations were performed with the molecular properties listed in Table 2. Structures and frequencies of alkyl iodides and alkyl radicals were estimated mainly from the published structures[24,25] and frequencies[26,27] of alkyl halides, alkanes, and alkyl radicals. Some unknown frequencies were estimated by ab initio calculations [at HF/3-21G or HF/6-31G(d) level] using the Gaussian 94 program.[28] Structures and the frequencies for the four-center HI elimination transition states were estimated from the published ab initio calculation results,[14] known structure, and group frequencies of each specific molecular moiety. Also some frequencies, which were difficult to estimate, were taken from the HF/3-21G level ab initio calculations. For alkyl radicals, the internal rotation of the alkyl group bonded to the radical center carbon was treated as a free

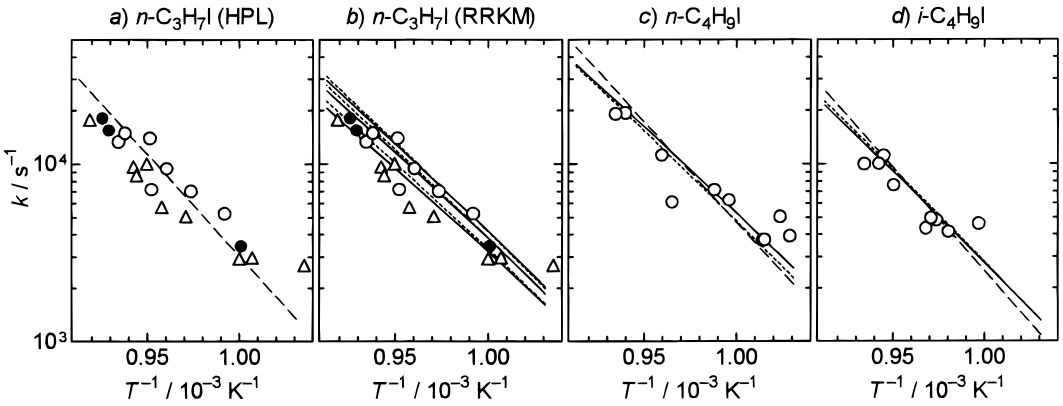

Figure 3. Observed and calculated overall thermal decomposition rate constants (k) for (a and b) n-C_3H_7I, (c) n-C_4H_9I, and (d) i-C_4H_9I. Dashed lines (- - -) denote the results of high-pressure limit analysis. Dotted lines (• • •) denote the results of single-channel RRKM analysis and solid lines (—) denote the results of two-channel RRKM analysis. Different symbols in (a) and b) denote the experimental data at different pressures: 0.64 atm (○), 1.24 atm (△), and 1.91 atm (●). Experimental data plotted in (a) and (b) are the same. In (a), the experimental data are compared with high-pressure limit analysis, while in (b), they are compared with RRKM analysis at pressures of 0.64, 1.24, and 1.91 atm (correspond to the lines from lower to upper).

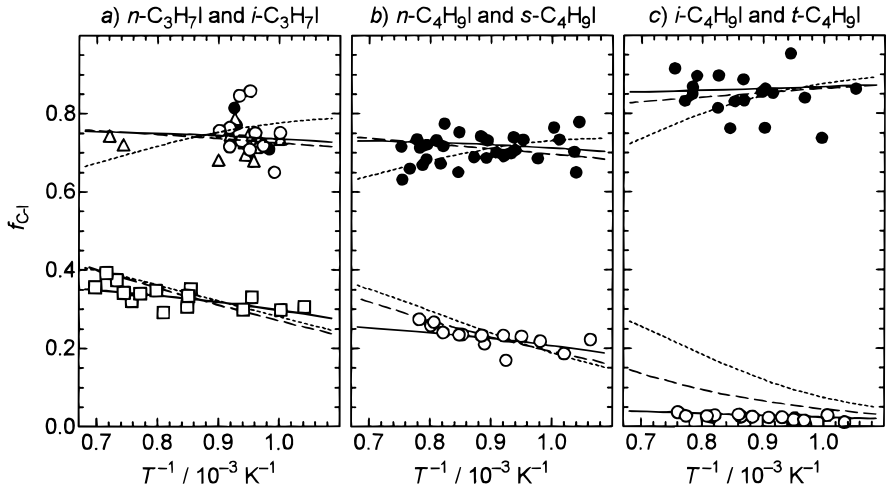

Figure 4. Observed and calculated branching fractions for C−I bond fission channels (f_{C-I}). (a) Branching fractions for n-C_3H_7I (○, △, ●,) and i-C_3H_7I (□). Different symbols for n-C_3H_7I denote the experiments at different pressures (same as in Figure 3). (b) Branching fractions for n-C_4H_9I (●) and s-C_4H_9I (○). (c) Branching fractions for i-C_4H_9I (●) and t-C_4H_9I (○). Dashed lines (- - -), dotted lines (• • •), and solid lines (—) denote the results of high-pressure limit analysis, single-channel RRKM analysis, and two-channel RRKM analysis, respectively.

TABLE 1: C-I Bond Dissociation Energies and Arrhenius *A*-Factors

molecule	D_{298}(C−I)[a]/ kJ mol^{-1}	A(C−I)[b]/s^{-1}	A(HI)[b]/s^{-1}	$(\sigma/n)_{HI-TS}^{-1}/(\sigma/n)_{RI}^{-1}$ [c]	A(HI)/ A(C−I)
C_2H_5I	231.7				
n-C_3H_7I	234.9	7.64×10^{14}	1.67×10^{14}	2/3	0.219
i-C_3H_7I	234.0	9.09×10^{14}	3.44×10^{14}	6/3	0.378
n-C_4H_9I	230.8	8.87×10^{14}	1.98×10^{14}	2/3	0.223
s-C_4H_9I	237.5	1.01×10^{15}	4.42×10^{14}	5/3	0.438
i-C_4H_9I	233.0	9.47×10^{14}	3.53×10^{14}	1/3	0.373
t-C_4H_9I	224.4	9.74×10^{14}	3.58×10^{14}	9/3	0.368

[a] C−I bond dissociation energy at 298 K calculated from the literature[20−23] heats of formation of alkyl iodides, alkyl radicals, and iodine atom. [b] A(C−I) and A(HI) denote the preexponential factors for C−I bond fission and HI elimination channels, respectively. These were derived from the Arrhenius plot of the calculated high-pressure limit rate constants in the temperature range 900−1400 K. [c] Statistical factor for the HI elimination channel, that is, a total correction factor for rotational symmetry number and number of optical isomers and/or rotational conformers. This is, of course, proportional to the intuitive "reaction path degeneracy", which is 2, 6, 2, 5, 1, and 9, respectively, from n-C_3H_7I through t-C_4H_9I.

rotator since the barrier height for such an internal rotation was known to be very low (~1 kJ mol^{-1}).[29] Other internal torsion modes were treated as vibrations. The rotational symmetry number, σ, listed in the table includes the symmetry number of internal free rotators. For s-C_4H_9I, two distinct transition states are possible, leading to the formation of 1-C_4H_8 and 2-C_4H_8. Since the properties for these two transition states are quite similar to each other, these two were merely counted as the "isomers" in the calculation. As a check of the validity of the estimations, entropy was calculated for alkyl iodides and alkyl radicals from the properties listed in Table 2. The calculated entropy agrees well with the experimental value,[22] as well as that estimated by the group additivity method[30] within ±6.0 J K^{-1} mol^{-1}.

A variational approach was applied to the simple C−I bond fission channel. The potential energy curve for the C−I bond was approximated by the Morse function,

$$V(r) = D_e\{1 - \exp[\beta(r_e - r)]\}^2 \qquad (12)$$

with $\beta = 2.4$ Å^{-1} and $r_e = 2.17$ Å for all alkyl iodides. Variation of the adiabatic vibrational frequencies was estimated by the interpolation between the alkyl iodide and the alkyl radical by the formula proposed by Quack and Troe,[31]

$$\nu(r) = [\nu(r_e) - \nu(r_\infty)] \exp[\alpha(r_e - r)] + \nu(r_\infty) \qquad (13)$$

TABLE 2: Molecular Properties Used in the Calculations

	RI			R			HI elimination TS		
R	σ/n[a]	rot. consts/cm^{-1}	vib freq[b]/cm^{-1}	σ/n	rot. consts/cm^{-1}	vib freq[b]/cm^{-1}	σ/n	rot. consts/cm^{-1}	vib freq[b]/cm^{-1}
n-C_3H_7	1/3	0.81410, 0.04442, 0.04316	3000(7), 1430(3), 1350(3), 1280(3), 1050(2), 940(2), 760(2), 500, 360, 240, 200, 90	2	1.0170, 0.3080, 0.2749	3000(7), 1430(4), 1350(3), 1050(2), 1030(2), 780, 760, 540, 360, 240, −10	1/2	0.31340, 0.03980, 0.03693	3000(6), 1700, 1450, 1430(3), 1310(3), 1120, 1090(2), 1050(2), 930, 570, 390, 250, 170(2), 85
i-C_3H_7	1	0.28029, 0.07280, 0.06135	3000(7), 1430(6), 1260(2), 1050(4), 940(2), 500, 360, 290, 240(2), 200	18	1.2198, 0.2766, 0.2465	3000(7), 1430(6), 1300, 1050(4), 1030(2), 370, 360, −6(2)	1/2	0.26759, 0.04534, 0.04069	3000(6), 1770, 1430(3), 1370(4), 1090(2), 1050(4), 460, 390, 380, 200, 170, 85
n-C_4H_9	1/9	0.48616, 0.02528, 0.02447	3000(9), 1430(3), 1350(6), 1280(3), 1050(2), 940(3), 760(3), 500, 360(2), 240, 200, 90(2)	2/3	0.8067, 0.1326, 0.1250	3000(9), 1430(4), 1350(6), 1050(2), 1030(3), 780, 760(2), 540, 360(2), 240, 90, −9.7	1/6	0.15228, 0.02961, 0.02578	3000(8), 1700, 1450, 1430(3), 1350(3), 1310(3), 1120, 1090(3), 1050(2), 930, 760, 570, 390(2), 240, 160, 130, 110, 60
s-C_4H_9	1/6	0.12808, 0.06035, 0.04331	3000(9), 1430(6), 1350(3), 1260(2), 1050(4), 940(3), 760, 500, 360(2), 290, 240(2), 200, 90	3	0.7997, 0.1260, 0.1192	3000(9), 1430(6), 1350(3), 1300, 1050(4), 1030(3), 760, 370, 360(2), 240, −1.4, −5.6	1/10	0.12174, 0.03521, 0.02850	3000(8), 1700, 1430(6), 1370, 1310(3), 1200, 1090(3), 1050(4), 460, 390(2), 200, 170, 160, 110, 60
i-C_4H_9	1/3	0.26383, 0.03823, 0.03488	3000(9), 1430(6), 1330(2), 1280(3), 1050(4), 940(3), 760, 500, 490, 360(2), 240(2), 200, 90	2	0.2855, 0.2749, 0.1610	3000(9), 1430(7), 1330(2), 1050(4), 1030(3), 780, 540, 490, 360(2), 240(2), −9.7	1	0.17003, 0.02922, 0.02850	3000(8), 1610, 1450, 1430(6), 1140, 1120, 1090(3), 1050(4), 930, 570, 440, 390(2), 250, 170(2), 110, 60
t-C_4H_9	3	0.15816, 0.05208, 0.05208	3000(9), 1430(9), 1050(6), 940(3), 500, 490, 360(2), 240(3), 200(2)	162	0.2628, 0.2628, 0.1420	3000(9), 1430(9), 1050(6), 1030(3), 360(2), 270, −5.6(3)	1	0.15014, 0.03396, 0.03351	3000(8), 1770, 1430(6), 1370(3), 1090(3), 1050(6), 440, 390(2), 380, 200(2), 110, 60

[a] σ denotes the symmetry number of external and internal rotations, and n denotes the number of optical isomers and/or rotational conformers. [b] Values in parentheses are degeneracy of vibrations. Negative frequencies denote the free rotators, and the absolute values are the rotational constants.

with $\alpha = 1.0$ Å^{-1} recommended for many reactions. For the vibrational mode correlating to the free rotation in the products, the partition function was interpolated with the formula[31]

$$Q(r) = [Q(r_e) - Q(r_\infty)] \exp[\gamma(r_e - r)] + Q(r_\infty) \quad (14)$$

with $\gamma = 0.75$ Å^{-1}. The location of the transition state was determined so as to minimize the rate constant calculated by TST at each temperature, according to the canonical variational TST or the maximum free energy criterion.[31]

The calculated Arrhenius preexponential factors (*A*-factors) are listed in Table 1. From simple intuition, the *A*-factor can be expected to be proportional to the statistical factor (or the reaction path degeneracy) which is unity for all the C−I bond fission channels, and is 1/3−9/3 for the HI elimination channel, as shown in Table 1. However, the calculated *A*-factors show smaller difference among primary, secondary, and tertiary iodides. It should be noted that the ratio of the partition functions of the transition state and the reactant, Q^*/Q, for the HI elimination process mainly reflects the statistical factor at lower temperatures. For example, $(Q^*/Q)[t\text{-}C_4H_9I]/(Q^*/Q)[i\text{-}C_3H_7I]$ is 1.405 and 1.695 at 1200 and 700 K, respectively, for which the ratio of the statistical factor is 1.5. However, in the *A*-factor, this difference was canceled with the larger temperature dependence of Q^*/Q for *i*-C_3H_7I. For example, $A[t\text{-}C_4H_9I]/A[i\text{-}C_3H_7I] = 1.04$ and 1.18 at 900−1400 K (Table 1) and at (600−800 K). The latter is in good agreement with the *A*-factors reported by Tsang,[8] $A[t\text{-}C_4H_9I]/A[i\text{-}C_3H_7I] = 10^{13.73}/10^{13.67} = 1.15$ at around 700 K. As a general trend, the temperature dependence of Q^*/Q is larger in the order primary > secondary > tertiary iodides. For these reasons, the effect of the *A*-factor was small and the maximum difference in A(HI)/A(C−I) was only a factor of 2 among all iodides as shown in Table 1. The main cause of the drastic change in the branching fraction should be attributed to the activation energies.

For primary iodides, the threshold energies for the C−I bond fission channel, E_0(C−I), and those for the four-center HI elimination channel, E_0(HI), were derived by the best fit to the experimental overall rate constants [which is essentially sensitive to the E_0(C−I)] and the branching fractions [which is sensitive to the difference of the threshold energies, E_0(C−I) − E_0(HI)]. The derived D_0(C−I) [C−I bond dissociation energy at 0 K] and E_0(HI) are [in kJ mol^{-1} unit] as follows: 227.6 and 207.8 for *n*-C_3H_7I, 226.0 and 205.1 for *n*-C_4H_9I, and 230.3 and 218.7 for *i*-C_4H_9I. Since overall rate constants could not be measured for secondary and tertiary iodides, D_0(C−I) was assumed to be 228 kJ mol^{-1}, which is the averaged value of D_0(C−I) for primary iodides determined by the best fit to the experimental rate constants. For *t*-C_4H_9I, the E_0(HI) was determined so as to reproduce the overall rate constants reported by Hippler et al.,[17] since the observed branching fraction may be overestimated for the reason described above. The derived E_0(HI) values are [in kJ mol^{-1} unit] as follows: 193.0 for *i*-C_3H_7I, 190.2 for *s*-C_4H_9I, and 173.1 for *t*-C_4H_9I. As a general trend, E_0(HI) decreases from primary (∼211 kJ mol^{-1}) to secondary (∼192 kJ mol^{-1}), and further to tertiary (∼173 kJ mol^{-1}) iodide.

The results of the high-pressure limit analysis are shown in Figures 3 and 4 by dashed lines (- - -). The predicted rate constants assuming the high-pressure limit does not satisfactory reproduce the temperature dependence, especially that of the branching fraction for secondary and tertiary iodides. The E_0(HI) for t-C_4H_9I determined from the rate constants by Hippler et al.[17] is inconsistent with the present very small f_{C-I}, <0.05, under the assumption of high-pressure limit. Detailed falloff analysis seems to be necessary in order to explain our experimental data, and in order to derive the reliable threshold energies.

B. RRKM Analysis. The failure of the high-pressure limit analysis suggests two possibilities. (1) The falloff effect is large and different between the two channels. (2) The mutual effect of the two channels is large. To investigate the two problems separately, two kinds of RRKM calculations were performed. The first is an RRKM calculation with proper treatment of the falloff effect but where two channels were treated independently, and the second is an RRKM calculation with the proper treatment of both falloff and mutual effects. The RRKM calculations were performed by using the UNIMOL program suit.[32] In this program, the steady-state internal energy distribution was calculated as the numerical solution to the eigenvalue problem of the master equation. In the RRKM calculation, the location of the transition state for the C−I bond fission channel was fixed at the position determined from the variational treatment at 1200 K. In the present experimental temperature range, 950−1400 K, the high-pressure rate constants calculated with this fixed TS approach differ not more than 5% from the full variational treatment. Collisional energy transfer was assumed to obey the exponential-down model.

Again, the threshold energies, E_0(C−I) and E_0(HI), were derived from the best fit to the experimental results. The results of the two types of the RRKM calculations were compared with experimental results in Figures 3 and 4. The single-channel RRKM calculation, in which two channels are treated independently but the falloff effect was properly included, does not reproduce the experimental temperature dependence. On the other hand, the multichannel RRKM calculation, in which the mutual effects of the two channels are treated properly, well reproduces the experimentally observed temperature dependence. Further, this multichannel calculation also reproduces the f_{C-I} for t-C_4H_9I, for which the E_0(HI) was determined by the best fit to the rate constants reported by Hippler et al.[17] With the threshold energies derived from the multichannel RRKM analysis, the calculated high-pressure limit rate constants also well reproduce the lower temperature rate constants reported by Tsang[8] for i-C_3H_7I and t-C_4H_9I within ±40%. These consistencies also confirm the validity of the present measurement and the multichannel RRKM analysis. The calculated product of microcanonical rate constant and internal population in the RRKM calculation is shown in Figure 5. Not only the high-pressure limit calculation but also the single-channel calculation with only the higher C−I bond fission channel apparently overestimate the rate constants since they do not include the population depletion by the lower channel.

In the RRKM calculation, the value of the average downward energy transferred per collision, $\langle\Delta E_{down}\rangle$, was set to be 600 cm^{-1} and assumed to be temperature independent. Change in the $\langle\Delta E_{down}\rangle$ affects the overall rate constants to some extent, approximately a similar extent as the pressure effect as shown in Figure 3. However, the large change in $\langle\Delta E_{down}\rangle$ affects the calculated branching fractions only very slightly over $400 \le \langle\Delta E_{down}\rangle \le 900$ cm^{-1}, and the effect was always less than 1%.

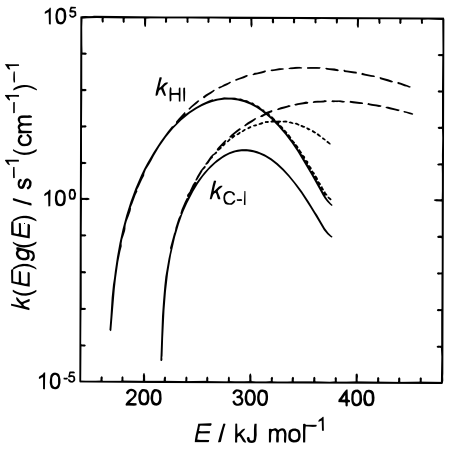

Figure 5. Product of microcanonical rate constant [$k(E)$] and internal population [$g(E)$] calculated for t-C_4H_9I at 1300 K and 0.6 atm. Dashed lines (- - -), dotted lines (· · ·), and solid lines (- - -) denote the calculation assuming the high-pressure limit, maser equation calculation with single exit channel, and that with two exit channels, respectively.

Experiments under a much wider pressure range, especially extended to lower pressures, will be necessary to extract the $\langle\Delta E_{down}\rangle$ from the experiments. Although the present experimental results were not sensitive to the quantity $\langle\Delta E_{down}\rangle$, it should be noted that the multichannel treatment is still essential to explain the present experimental results obtained at rather high pressures where the pressure dependence of the overall rate constants was found to be small.

Similarly, the pressure effect was found to be small in the present experimental conditions. Although the largest pressure effect to the calculated overall rate constant (for primary iodides) was found for n-C_3H_7I, as shown in Figure 3b, experimental investigation could not reveal this effect. The pressure effect to the branching fraction was calculated to be very small, typically +0.005 and at maximum +0.019 when the pressure was doubled, and thus, no experimental investigation on the pressure effect was intended other than for n-C_3H_7I.

C. Threshold Energies and the Nature of the Transition State. Table 3 summarizes the derived threshold energies from the multichannel RRKM analysis. For primary iodides (n-C_3H_7I, n-C_4H_9I, and i-C_4H_9I), the threshold energy for the C−I bond fission channel [E_0(C−I)] was derived from the best fit to the experimental rate constants and its error limit was estimated to be ±7.3 kJ mol^{-1}. The bond dissociation energy at 0 K (D_0) was derived by assuming the Morse potential curve, and that at 298 K (D_{298}) was derived by correcting the thermal energy calculated from the properties listed in Table 2. For the secondary and tertiary iodides, the bond dissociation energy (D_0) was assumed to be 223.7 kJ mol^{-1}, which is the average for primary iodides. The derived bond dissociation energies agree well with those calculated from the heats of formation in the literature, considering the error limit in the present experimental value (±7.3 kJ mol^{-1}) and those in the heats of formation (±4−8 kJ mol^{-1}). For t-C_4H_9I, the threshold energy for the HI elimination channel [E_0(HI)] was derived by the best fit to the direct experimental measurements by Hippler et al. This E_0(HI) and the estimated E_0(C−I) well reproduce the present branching fraction for t-C_4H_9I. This fact also suggests the validity of the assumption of the common bond dissociation energy for primary and tertiary iodides. The carbon−halogen bond dissociation energies have been discussed in relation to the four-center elimination reactions and are known to be almost independent of the α-CH_3 substitution.[5] Because of the electron-withdrawing nature of the halogen atom, the α-CH_3 substitution

TABLE 3: Threshold Energies Derived from the Multi-Channel RRKM Analysis

	present threshold energy[a]/kJ mol^{-1}			lit threshold energy/kJ mol^{-1}			C−I bond dissoc energy/kJ mol^{-1}		
molecule	E_0(C−I)	E_0(HI)	ΔE_0	E_0(C−I)	E_0(HI)	ref	D_0[b]	D_{298}[b]	D_{298}(lit.)[c]
C_2H_5I				218.8	203.8	18			231.7
n-C_3H_7I	216.7	202.1	−14.6	217.6	198.7	16	222.3	226.1	234.9
i-C_3H_7I	(217.0)	190.8	−26.2		185.8	16	(223.7)[d]	(227.4)	234.0
n-C_4H_9I	216.3	201.7	−14.6				222.1	225.9	230.8
s-C_4H_9I	(216.5)	188.3	−28.2				(223.7)[d]	(226.7)	237.5
i-C_4H_9I	220.5	214.2	−6.3				226.6	230.4	233.0
t-C_4H_9I	(216.3)	168.6	−47.7				(223.7)[d]	(226.8)	224.4

[a] E_0(C−I) and E_0(HI) denote the threshold energies for the C−I bond fission channel and that for the four-center HI elimination channel, respectively. ΔE_0 is the difference of threshold energies [$=E_0$(HI) − E_0(CI)]. [b] D_0 was derived from E_0(CI) by assuming the Morse potential function. D_{298} was evaluated from D_0 by calculating the thermal energy from the properties listed in Table 1. [c] Literature bond dissociation energies same as those listed in Table 1. [d] D_0 for secondary and tertiary iodides are assumed to be the constant, 223.7 kJ mol^{-1}, which is the average of D_0 derived for primary iodides. E_0(C−I) and D_{298} values in parentheses were calculated from the constant D_0.

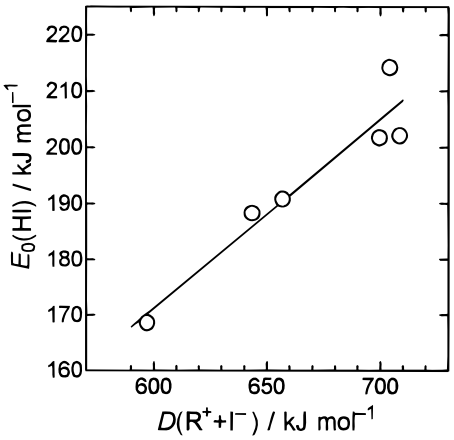

Figure 6. A correlation between the ion dissociation energy for RI → $R^+ + I^-$ [D(R^++I^-)] and the threshold energy for the four-center HI elimination process. Solid line is the result of a simple least-squares fit.

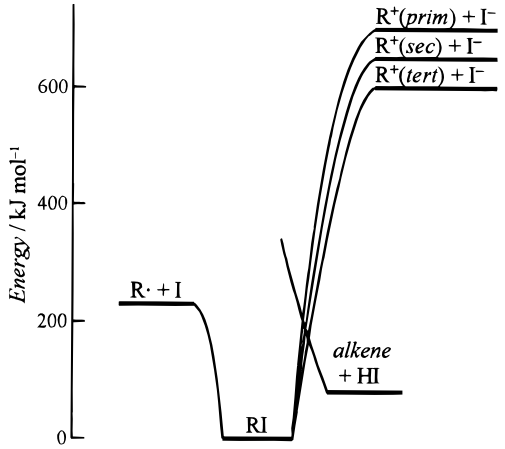

Figure 7. Hypothetical interpretation for the α-CH_3 substituent effect on the barrier height for the four-center HI elimination process. The avoided intersection between the ionic dissociation surface and the repulsive surface of the HI approach to the double bond is expected to be the origin of the four-center elimination transition state.

probably stabilizes the alkyl halides by an amount almost equal to the stabilization of alkyl radicals. This effect results in the almost constant C−I bond dissociation energies for the primary, secondary, and tertiary iodides.

The branching fraction observed in the present study is a sensitive measure of the difference of threshold energies (ΔE_0) between C−I bond fission and HI elimination channels. The accuracy of the ΔE_0 is estimated to be ±4.0 kJ mol^{-1}, while that for absolute threshold energies is poorer, ±7.3 kJ mol^{-1}. The derived threshold energies for *n*-C_3H_7I and *i*-C_3H_7I agree well with those reported by King et al.[16] The threshold energies (for both the C−I fission and HI elimination channels) derived for primary iodides are close to each other and also close to those derived for C_2H_5I by Kumaran et al.[18] The E_0(HI) was found to decreases by ∼14 kJ mol^{-1} from primary to secondary iodides and by ∼20 kJ mol^{-1} from secondary to tertiary iodides. These differences were also in agreement with the difference of activation energy derived in earlier studies[5,8] (∼29 kJ mol^{-1} or 25 ± 4 kJ mol^{-1} per each α-CH_3 substitution) if we consider the difference between the activation energy (E_a) and the threshold energy (E_0). A high-pressure limit calculation around 1000 K indicates that the $E_a - E_0$ is ∼10, ∼7, and ∼4 kJ mol^{-1} for primary, secondary, and tertiary iodides.

The threshold energies for HI elimination channels are plotted in Figure 6 against the heterolytic dissociation energies for RI → $R^+ + I^-$ according to the indication in the earlier studies.[4] A clear correlation was found. Although the semi-ion-pair model[5] has been shown to be successful for the explanation of the many four-center HX elimination reactions with minor modification, the cause of the charge separation in the transition state has not been well understood. Maccoll presented a picture of the perturbation from the "ionic excited state" to the transition state and the exit potential surface to HX + olefin (Figure 6 of ref 4) from the analogy to the S_N1 or E_1 reactions in a polar solvent. However, our preliminary ab initio (at HF/3-21G level) analysis of charge separation along the four-center elimination IRC indicates that the charge separation increases from reactant to TS, starts to decrease around TS, and suddenly disappears in the exit channel. The charge separation character was seen in the alkyl iodide side but not in the HI + olefin side as indicated by Maccoll.

A simple interpretation for the correlation between the threshold energy and the heterolytic dissociation energy is illustrated in Figure 7. Probably, the heterolytic ion dissociation potential energy surface intersects with the repulsive, nonpolar potential surface of the HI approach to the double bond. The avoided intersection of these two surfaces is expected to be the origin of the transition state for HI elimination. The lowering of the ultimate heterolytic dissociation energy decreases the ion dissociation potential surface, while the repulsive potential does not change a lot. In this assumption, similar to the Evans−Polanyi rule, the lowest point of the intersection of the two surfaces is expected to decrease as the ion dissociation energy decreases. Recent ab initio calculation[14] for the F− and Cl− substituent effects on HCl or HF elimination transition states showed that there is no obvious connection between the barrier height and atomic charges. But, one point should be noted; the Mulliken population analysis at the transition state only may

not be enough to resolve the full feature of the transition state since the transition state would be a critical point along the IRC where the charge distribution suddenly changes because of the avoided intersection of very ionic and nonpolar surfaces. Further, F− or Cl− substituent effects are rather complex, since they involve both σ electron withdrawal and π electron donation from lone pairs. The CH_3− substitution seems to be simpler since the σ electron donation is expected to be the dominant effect.

Also, there is a question whether the ground state of alkyl halide diabatically correlates to the ion pair ($R^+ + I^-$). From the large electronegativity of the halogen atoms, some ionic character of the carbon−halogen bond is expected. The almost constant bond dissociation energy for carbon−halogen bond for primary, secondary, and tertiary alkyl halides suggests the ionic stabilization of the alkyl halides by α-CH_3 substitution. If the ground-state alkyl halide diabatically correlates to the ion pair ($R^+ + I^-$), the avoided intersection between the ionic and covalent surfaces is expected even in the simple C−X bond fission potential energy surface. Our preliminary HF/3-21G level ab initio calculation also suggests the avoided intersection between the ionic and covalent surfaces along the simple C−X bond fission channel. Probably, the ground state alkyl iodide diabatically correlates the ion pair ($R^+ + I^-$), and the avoided intersections produce both reaction coordinates to simple R−I bond fission and HI elimination. However, this hypothetical interpretation should be examined with detailed, higher level ab initio calculations.

Conclusion

In the present study, the branching fractions for the simple C−I bond fission and four-center HI elimination processes were measured for a series of alkyl iodides at temperatures of 950−1400 K and at pressures around 1.0 atm. The overall rate constants were also measured for primary iodides at temperatures of 950−1100 K. The drastic change in the branching fractions for primary, secondary, and tertiary iodides was mainly ascribed to the change of the threshold energy for HI elimination processes. An RRKM analysis showed that the mutual effect of the two dissociation channel is essentially important. A simple interpretation for the α-CH_3 substituent effect on the threshold energy for the HI elimination channel was presented in terms of the avoided intersection between ionic and nonpolar potential energy surfaces.

References and Notes

(1) Quick, C. R.; Wittig, C. *J. Chem. Phys.* **1980**, *72*, 1694.

(2) Molina, M. J.; Pimentel, J. *J. Chem. Phys.* **1972**, *56*, 3988 and references therein.

(3) Sudbø, Aa. S.; Schulz, P. A.; Shen, Y. R.; Lee, Y. T. *J. Chem. Phys.* **1978**, *69*, 2312 and references therein.

(4) Maccoll, A. *Chem. Rev.* **1969**, *69*, 33.

(5) Benson, S. W.; Bose, A. N. *J. Chem. Phys.* **1963**, *39*, 3463.

(6) Maccoll, A.; Thomas, P. J. *Nature* **1955**, *176*, 392.

(7) Benson, S. W.; Haugen, G. R. *J. Am. Chem. Soc.* **1965**, *87*, 4036.

(8) Tsang, W. *J. Chem. Phys.* **1964**, *41*, 2487.

(9) (a) Tschuikow-Roux, E.; Quiring, W. J.; Simmie, J. M. *J. Phys. Chem.* **1970**, *74*, 2449. (b) Tschuikow-Roux, E.; Quiring, W. J. *J. Phys. Chem.* **1971**, *75*, 295.

(10) (a) Maltman, K. R.; Tschuikow-Roux, E.; Jung, K.-H. *J. Phys. Chem.* **1974**, *78*, 1035. (b) Tschuikow-Roux, E.; Maltman, K. R. *Int. J. Chem. Kinet.* **1975**, *7*, 363.

(11) (a) Hassler, J. C.; Setser, D. W. *J. Chem. Phys.* **1966**, *45*, 3246. (b) Johnson, R. L.; Setser, D. W. *J. Phys. Chem.* **1967**, *71*, 4366. (c) Dees, K.; Setser, D. W. *J. Chem. Phys.* **1968**, *49*, 1193. (d) Chang, H. W.; Setser, D. W. *J. Am. Chem. Soc.* **1969**, *91*, 7648. (e) Kim, K. C.; Setser, D. W. *J. Phys. Chem.* **1974**, *78*, 2166.

(12) Jones, Y.; Holmes, B. E.; Duke, D. W.; Tipton, D. L. *J. Phys. Chem.* **1990**, *94*, 4957.

(13) Kato, S.; Morokuma, K. *J. Chem. Phys.* **1980**, *73*, 3900.

(14) Toto, J. L.; Pritchard, G. O.; Kirtman, B. *J. Phys. Chem.* **1994**, *98*, 8359.

(15) Just. Th.; Troe, J. *J. Phys. Chem.* **1980**, *84*, 3068.

(16) King. K. D.; Golden, D. M.; Spokes, G. N.; Benson, S. W. *Int. J. Chem. Kinet.* **1971**, *3*, 411.

(17) Hippler, H.; Riedl, A.; Troe, J.; Willner, J. *Z. Phys. Chem.* **1991**, *171*, 161.

(18) Kumaran, S. S.; Su, M.-C.; Lim, K. P.; Michael, J. V. *Proc. Symp. (Int.) Combust.* **1996**, *26*, 605.

(19) Koshi, M.; Yoshimura, M.; Fukuda, K.; Matsui, H.; Saito, K.; Watanabe, M.; Imamura, A.; Chen, C. *J. Chem. Phys.* **1990**, *93*, 8703.

(20) Atkinson, R.; Baulch, D. L.; Cox, R. A.; Hampson, R. F., Jr.; Kerr, J. A.; Troe, J. *J. Phys. Chem. Ref. Data* **1992**, *21*, 1125.

(21) Domalski, E. S.; Hearing, E. D. *J. Phys. Chem. Ref. Data* **1993**, *22*, 805.

(22) Stein, S. E. *NIST Structure and Properties*, version 2.0; National Institute of Standards and Technology: Gaithersburg, 1994.

(23) Frenkel, M.; Marsh, K. N.; Wilhoit, R. C.; Kabo, G. J.; Roganov, G. N. *Thermodynamics of Organic Compounds in the Gas State*; Thermodynamics Research Center: College Station, 1994.

(24) Harmony, M. D.; Laurie, V. W.; Kuczkowski, R. L.; Schwendeman, R. H.; Ramsay, D. A.; Lovas, F. J.; Lafferty, W. J.; Maki, A. G. *J. Phys. Chem. Ref. Data* **1979**, *8*, 619.

(25) Kasuya, T.; Oka, T. *J. Phys. Soc. Jpn.* **1960**, *15*, 296.

(26) (a) Simanouchi, T. *Tables of Molecular Vibrational Frequencies*; National Bureau of Standards: Washington, DC, 1972; Consol. Vol. I. (b) Chen, S. S.; Wilhoit, R. C.; Zwolinski, B. J. *J. Phys. Chem. Ref. Data* **1975**, *4*, 859. (c) Kudchadker, S. A.; Kudchadker, A. P. *J. Phys. Chem. Ref. Data* **1979**, *8*, 519. (d) Sheppard, N. *Trans. Faraday Soc.* **1950**, *46*, 527. (e) Sheppard, N. *Trans. Faraday Soc.* **1950**, *46*, 533. (f) Ogawa, Y.; Imazeki, S.; Yamaguchi, H.; Matsumura, H.; Harada, I.; Shimanouchi, T. *Bull. Chem. Soc. Jpn.* **1978**, *51*, 748.

(27) (a) Pacansky, J.; Dupuis, M. *J. Am. Chem. Soc.* **1982**, *104*, 415. (b) Pacansky, J.; Brown, D. W.; Chang, J. S. *J. Phys. Chem.* **1981**, *85*, 2562. (c) Pacansky, J.; Chang, J. S. *J. Chem. Phys.* **1981**, *74*, 5539. (d) Pacansky, J.; Coufal, H. *J. Chem. Phys.* **1980**, *72*, 3298. (e) Pacansky, J.; Horne, D. E.; Gardini, G. P.; Bargon, J. *J. Phys. Chem.* **1977**, *81*, 2149.

(28) Frisch, M. J.; Trucks, G. W.; Schlegel, H. B.; Gill, P. M. W.; Johnson, B. G.; Robb, M. A.; Cheeseman, J. R.; Keith, T.; Petersson, G. A.; Montgomery, J. A.; Raghavachari, K.; Al-Laham, M. A.; Zakrzewski, V. G.; Ortiz, J. V.; Foresman, J. B.; Cioslowski, J.; Stefanov, B. B.; Nanayakkara, A.; Challacombe, M.; Peng, C. Y.; Ayala, P. Y.; Chen, W.; Wong, M. W.; Andres, J. L.; Replogle, E. S.; Gomperts, R.; Martin, R. L.; Fox, D. J.; Binkley, J. S.; Defrees, D. J.; Baker, J.; Stewart, J. P.; Head-Gordon, M.; Gonzalez, C.; Pople, J. A. *Gaussian 94*, revision E.1; Gaussian, Inc.: Pittsburgh, PA, 1995.

(29) Pacansky, J.; Schubert, W. *J. Chem. Phys.* **1982**, *76*, 1459.

(30) Benson, S. W. *Thermochemical Kinetics*, 2nd ed.; Wiley: New York, 1976.

(31) Quack, M.; Troe, J. *Ber. Bunsen-Ges. Phys. Chem.* **1977**, *81*, 329.

(32) Gilbert, R. G.; Smith, S. C.; Jordan, M. J. T. *UNIMOL program suite*, 1993 (calculation of falloff curves for unimolecular and recombination reactions). Available from the authors at School of Chemistry, Sydney University, NSW 2006, Australia, or by e-mail to gilbert_r@summer.chem.su.oz.au.